



Physical-controlled CO₂ effluxes from reservoir surface in the upper Mekong River Basin: a case study in the Gongguoqiao Reservoir

Lin Lin¹, Xixi Lu^{1,2}, Shaoda Liu³ and Kaidao Fu^{4,*}

¹Department of geography, National University of Singapore, 117570, Singapore

5 ²Inner Mongolia Key Lab of River and Lake Ecology, School of Ecology and Environment, Inner Mongolia University, Hohhot, Inner Mongolia, 010021, China

³Yale School of Forestry & Environmental Studies 195 Prospect Street New Haven, CT 06511, USA

⁴Asian International River Center, Yunnan University, Chenggong University City, Chenggong, Kunming, Yunnan, 650500, China

10

Correspondence to: Kaidao Fu(kdfu@ynu.edu.cn)

Abstract. Impounding has greatly altered carbon cycle in rivers. To quantify this effect, we measured CO₂ effluxes from a mountainous valley-type reservoir in the upper Mekong River (Lancang River in China) and compared with those from the pristine river channel. Evasion rates from reservoir surface was 408 mg m⁻² d⁻¹ and 305 mg m⁻² d⁻¹ in the dry season and rainy season respectively, much lower than those from river channel of 2168 mg m⁻² d⁻¹ and 374 mg m⁻² d⁻¹. Lower efflux in the rainy season deviated from the traditional theory that rainfalls can bring more organic carbon for mineralization and increase the efflux. The analysis found that efflux was closely related to the physical mixing process of inflow and reservoir water. The light overflow rich in CO₂ in dry season contact the atmosphere directly and release more gases while the underflow in warm wet season leaved insufficient time for mineralization and hardly support high efflux in surface water. Evasion rate at the downstream of the dam was also limited due to surface water withdrawal. Lastly, the littoral zone was found to be a hotspot for CO₂ emission despite its limited area leading to its negligible contribution in total annual emission rate. In contrast, diurnal efflux variability in the littoral zone indicates that the effluxes were significantly higher at night than in the daytime, which increased the annual emission rate to by a half.

20

1 Introduction

25 Supersaturation of CO₂ in the inland waters (Cole et al., 1994) resulted in 0.75 to 2.12 Pg of carbon outgassing to the atmosphere annually (Battin et al., 2009; Cole et al., 2007; Raymond et al., 2013; Tranvik et al., 2009). Loss of carbon to the atmosphere from inland waters has been recognized as an important part of the carbon cycle which is confronting great anthropogenic impacts at the same time (Maavara et al., 2017; Regnier et al., 2013). Damming rivers to build large reservoirs for water supply, irrigation, hydroelectricity and flood controls is one of the most drastic changes in inland waters (Lehner & Döll, 2004; Varis et al., 2012). By flooding large area of forests, soils and different kinds of organic matter, reservoirs have

30



been identified as a large potential carbon source to the atmosphere since last century and caused a serious perturbation on the global carbon budget (Fearnside, 1997; Kelly et al., 1994; Rudd et al., 1993) as they not only enlarge water surface, but also produce more greenhouse gases (GHGs) than the natural waterbodies (Lima et al., 1998). Since carbon dioxide accounts for the largest proportion of GHGs emissions from the reservoirs, measurement of the areal emission rates has become an urgent task (Deemer et al., 2016; Mendonça et al., 2012).

Efforts have been made to evaluate CO₂ emissions from reservoir surfaces over the past decade (Deemer et al., 2016; Raymond et al., 2013; Varis et al., 2012; Vincent et al., 2000). The accumulated case studies indicated that CO₂ emission rates exhibited great seasonal variability and spatial heterogeneity (Barros et al., 2011; Deemer et al., 2016). Water temperature and quantity and quality of DOC have been regarded as the most important factors that control the CO₂ fluxes from reservoirs (Barros et al., 2011; Mendonça et al., 2012; Tadonleke et al., 2012). However, most of the existing studies concentrated in the North Europe, South America and North America, while few measurements of CO₂ effluxes were implemented in China, the country owns most of the reservoirs in the world and requires these effluxes urgently to gain green credits for its hydroelectric reservoirs.

Despite the limited dataset, the effluxes estimated from pCO₂ gradients found that most of the effluxes from Chinese reservoirs were much lower than that from tropical and boreal reservoirs (Li & Zhang, 2014a; Li et al., 2015) and the intense emissions shortly after impoundments resulted from trophic upsurge (Gunkel, 2009) were less significant than other regions (Ran et al., 2011). Analysis of the pCO₂ along the river continuum found lower effluxes in the reservoir center (Gao et al., 2017; Mei et al., 2011) as the pCO₂ in reservoir surface was subject to the biogeochemical processes of phytoplankton. The pCO₂ and effluxes from reservoirs were regulated by the balance between respiration and photosynthesis and quite sensitive to the monsoon climate (Guo et al., 2011; Mei et al., 2011; Zhao et al., 2011). Particularly, the Three Gorges Reservoir, one of the largest reservoir in China, attracted much attention for its high GHG emissions from the seasonally flooding littoral zone (Chen et al., 2009; Yang et al., 2012) and the algae bloom in the stagnant tributaries resulted from heavy eutrophication, which could lead to undersaturation of CO₂ in surface water (Ran et al., 2011; Wei et al., 2016; Yang et al., 2013; Zhao et al., 2013), turn the fluxes into negative and thus reverse the whole carbon budget (Guo et al., 2011; Pacheco et al., 2014; Tao, 2017).

The research above focuses on the reservoirs in the highly populated eastern plain where the waterbody is suffering from heavy eutrophication (Li & Zhang, 2014b; Mei et al., 2011; Ye et al., 2014). Given the spatial heterogeneity of CO₂ effluxes (Li & Zhang, 2014a), the case might be different in the less populated southwestern China where two thirds of the exploitable hydropower were found and many more reservoirs are being built (Hu & Cheng, 2013). In a region that was less populated, it was expected to see less carbon input from the catchments could result in less CO₂ production in the heterotrophic valley-type reservoirs (Huttunen et al., 2002; Roland et al., 2010; Tadonleke et al., 2012). Thus, this research aims to measure the CO₂ evasion with static chamber methods and analyze the spatial heterogeneity, seasonal variation and diurnal variation of the CO₂ efflux in the uppermost reservoir in the Lancang cascade reservoirs, in order to shed some light on the mechanism that controls the CO₂ effluxes and build the steps for clarification on the damming effect on carbon cycle.



2 Methods

2.1 Study area

The Gongguoqiao Reservoir (GGQ) is located in the Gongguo Town (Fig. 1, 25°35'9.87"N, 99°20'5.55"E) of Dali Prefecture (Yunnan, China) and has been the farthest upstream cascade reservoir in the upper Mekong River Basin by the end of 2016. Following the Xiaowan Reservoir right at downstream, GGQ was impounded in 2012. The Miaowei Reservoir at its upstream, was completed at the end of 2016. The backwater area stretches 44.3 km along the mainstream and 7 km along the tributary, the Bijiang River respectively. The width of the reservoir ranges from 110 to 120m in the dry season. The standard water level is 1307m, corresponding to the storage of 0.316 billion m³. But due to the small operating capacity (49 million m³), the reservoir is daily-operated. Thus, the water level fluctuates frequently and the average water retention time was no more than four days. The reservoir is mainly for hydropower production and generates 4.041 billion kW/h annually. With a catchment area of 97,200 km², around 32 billion m³ of water flows into the reservoir annually. As the reservoir is under the control of subtropical monsoon climate, the rainfalls in the rainy season spanning from May to October, account for 78.6% of the annual water discharge and 95% of the annual sediment discharge (21.51 million tons).

2.2 Study methods

2.2.1 Sampling

Five sampling points were selected along the mainstream and two were from the Bijiang River, a turbid tributary joining the reservoir about 1km right before the dam (Fig. 1). For comparison two points were in the river channel where water was flowing (Point R1 in the mainstream Mekong River and Point R2 in the tributary) and one was selected at the downstream of the dam (Point D). All the other points (P1-P4) in the reservoir has no flow velocity in surface water. However, due to serious silting on the relatively flat platform, Point L has become wetland suffering frequent flooding and draining as large area will be exposed to the air at the low water level when the water was discharged. Hence Point L was defined as littoral zone with daily flooding owing to the frequent fluctuation of the water levels. Point P2 to P4 were classified as pelagic zone. Sixteen campaigns were implemented from January to December 2016.

The effluxes were measured with a floating chamber connected to a non-dispersive infrared CO₂ analyzer (S157-P 0-2000ppm, Qubit, Canada) via the LQ-MINI interface (Vernier, USA). The chamber is a 20cm x 12cm x 10cm polypropylene rectangle translucent box inserted through a diamond-shape Styrofoam collar. The chamber will be turn upside down for three times to mix the gas within the box. Measurement of the CO₂ concentration did not begin until the reading of the analyzer became stable.

Calculation of effluxes was based on the slope of graph of concentration versus time in ppm/s according to methodology proposed by Tremblay et al. (2005). The equation was listed as Eq. 1:



$$Efflux = \frac{slope \times F1 \times F2 \times volume}{surface \times F3}, \quad (1)$$

In which F1 is the conversion factor from ppm to $\mu\text{g}/\text{m}^3$ (for CO_2 it was defaulted as 1798.45). F2 and F3 are the conversion factor from seconds to day (86400) and from μg to mg (1000) respectively. The volume refers to the air trapped in the chamber (m^3) and surface is the surface of the floating chamber over the water (m^2). The effluxes will be expressed in $\text{mg m}^{-2} \text{d}^{-1}$.

When the measurements of effluxes began, water temperature, pH, conductivity and dissolved oxygen (DO) were measured in situ with a portable multiparameter meter (Orion Star A, Thermo Scientific, USA). Air temperature and wind velocity were measured with a portable anemometer (GM8901, Benetech, China). For quality control, at least three water samples were collected from the 0.5m below the water surface with water bottles. For alkalinity, the water samples were titrated with 2M hydrochloric acid within 12 hours after collection. The alkalinity, pH and water temperature were used to calculate the partial pressure of CO_2 ($p\text{CO}_2$) with CO2SYS program (Lewis et al., 1998). The water samples were stored in 50ml centrifugal tubes and transported to the lab at a low temperature.

2.2.2 Laboratory analysis

The water samples for analysis of chlorophyll concentration were filtered with qualitative filter paper (80~120 μm) while the water samples for DOC analysis were filtered with 0.7 μm Whatman GF/F filters to remove the sediments. Concentration of chlorophyll was analyzed with a Phyto-PAM-II Multiple Excitation Wavelength Phytoplankton analyzer (Heinz Walz GmbH, Germany). The DOC analysis was conducted on the Vario TOC Analyzer (Elementar, Germany). Unfiltered water samples were analyzed with spectrophotometer (UV5500, Metash, China) after digestion with alkaline potassium persulfate and potassium persulfate for concentration of total nitrogen (TN) and total phosphorous (TP) according to HJ636-2012 (MEP, 2012) and GB11893-89 (MEP, 1989) respectively.

3 Results

3.1 Spatial and temporal variation of environmental factors

The water in riverine zone was characterized by low temperature, pH, nutrient concentration and high in alkalinity, conductivity, DOC concentration and chlorophyll, while the pelagic zone was filled with warm, more alkaline, eutrophic, but less aerobic water (Table 1). Water temperature ranged from 15.6 to 17.4 $^{\circ}\text{C}$, with an average of 16.8 $^{\circ}\text{C}$. The difference in water temperature between riverine zone and pelagic zone was no more than 2 $^{\circ}\text{C}$. Water temperature in the downstream of the dam was very close to the surface water upstream of the dam, suggesting that water passing the turbine should be drawn from the surface water instead of the bottom water which was supposed to be much cooler. The pH higher than 8.0 (averagely 8.46) suggested that water in the reservoir was alkaline without any significant spatial heterogeneity. Total alkalinity ranged from



2251 $\mu\text{mol/L}$ to 2666 $\mu\text{mol/L}$, with a mean value of 2441 $\mu\text{mol/L}$. Points located in the upstream had higher alkalinity than the downstream pelagic area with the maximum recorded in the littoral zone. Conductivity, ranging from 345 $\mu\text{S/cm}$ to 388 $\mu\text{S/cm}$ showed a similar variation trend as the alkalinity. Within the limited dataset, the free running water from inflow was more aerobic than the stagnant water. The dissolved oxygen concentration was approximately 4 mg/L higher than the pelagic area. Concentration of DOC was also significantly higher in the riverine zone while quite homogeneous in the other regions, possibly due to severe deposition. Both the concentration of TN and TP showed low values in the reservoir, with a mean value of 0.71 mg/L and 0.15 mg/L respectively. The maximum concentration of nutrients, however, was found in the littoral zones and pelagic area rather than in the riverine area on the mainstream. Low concentration of TN, TP and Chl a reveals the oligotrophic nature of the studied reservoir.

10 3.2 Spatial and seasonal variation of pCO_2

Most of the water samples had pCO_2 higher than the atmospheric value (410 μatm) and supersaturated with CO_2 (Table 1 & Fig. 2). This means that in most of time, the reservoir was supposed to be a CO_2 source to the atmosphere. The partial pressures recorded in this study ranged from 237 μatm to 14764 μatm , with an annual average of 919 μatm and median of 711 μatm . The values were close to the global average of artificial reservoirs (Raymond et al., 2013).

15 However, the annual pCO_2 of the reservoir ($703 \pm 407 \mu\text{atm}$) was comparable to the natural lakes in the Yunnan-Guizhou Plateau (639 μatm , Wang et al., 2003) when the pCO_2 from the river channel was excluded. The results was much lower than the pCO_2 of Lower Mekong River (Li et al., 2013). There was no data insofar from the origin of the Mekong River. But the research on three rivers on the Tibetan Plateau shows a median pCO_2 of 864 μatm , which was comparable to the values in the GGQ (Qu et al., 2017).

20 The pCO_2 in river channel was $852 \pm 1056 \mu\text{atm}$ and $733 \pm 232 \mu\text{atm}$ in the mainstream and the tributary respectively. These values were a little higher than the pCO_2 in the surface water of the pelagic zone, but the difference was insignificant ($p > 0.05$). pCO_2 showed no significant spatial heterogeneity in the reservoir in spring, summer and winter. The pCO_2 was below 800 μatm from May to August while increased drastically in late August. From September to April, the water level gradually increased and the pCO_2 fluctuated between 400 μatm to 1,200 μatm .

25 However, seasonal variation of the pCO_2 was significant ($p < 0.05$) as autumn showed a much higher pCO_2 than the other seasons. When the pCO_2 in both riverine zone and pelagic zone recorded their peak values, a significant decreasing trend toward downstream was found along the mainstream in autumn ($p < 0.05$) (Fig. 2). Frequent fluctuation of water level and continued rainfalls flushed plenty of deadwoods and organic matter to the reservoirs. Decomposition of the deadwoods and plants might acidify the water along the bankside, which finally lead to much higher pCO_2 in R1, P1 and L. Accumulation of deadwoods were most obvious in the littoral zone because the area was flat for deposition. The pCO_2 in the littoral zone was 14764 μatm and 11825 μatm in September and October respectively. Extremely high pCO_2 in the littoral zone indicates that this zone could be a potential “hotspot” for carbon emissions.



The $p\text{CO}_2$ measured at the downstream of the dam was quite stable throughout the year ($p > 0.50$), with an average of $658 \pm 176 \mu\text{atm}$. No drastic increase from P3 to D has been found throughout the year. The gradient in $p\text{CO}_2$ between P3, the point close to the dam and D ranged from $-247 \mu\text{atm}$ to $560 \mu\text{atm}$. Lower $p\text{CO}_2$ at the downstream of the dam than upstream was found from August to November. Unlike the cascade reservoirs on the Maotiao River which always recorded a higher $p\text{CO}_2$ at the downstream of the dam (Wang et al., 2011), the $p\text{CO}_2$ at the downstream of GGQ rarely reached $10,000 \mu\text{atm}$.

3.3 Spatial and seasonal variation of measured CO_2 effluxes

In Fig. 3 and Fig. 4, the CO_2 effluxes showed large spatial and seasonal variation in GGQ. The CO_2 effluxes ranged from -44 to $4952 \text{ mg m}^{-2} \text{ d}^{-1}$ in the whole reservoir, with a mean value of $352 \text{ mg m}^{-2} \text{ d}^{-1}$, or $8 \text{ mmol m}^{-2} \text{ d}^{-1}$. Only one negative value suggesting carbon absorption was found in P4. It confirms that the reservoir surface was a carbon source to the atmosphere.

The result was comparable to the results calculated from the $p\text{CO}_2$ with Thin Boundary Model, $344 \text{ mg m}^{-2} \text{ d}^{-1}$. However, the value was much lower than the estimated global average (Deemer et al., 2016; Holgerson & Raymond, 2016; Vincent et al., 2000). The annual effluxes at P1, P2, P3 and P4 was $465 \pm 529 \text{ mg m}^{-2} \text{ d}^{-1}$, $331 \pm 94 \text{ mg m}^{-2} \text{ d}^{-1}$, $336 \pm 92 \text{ mg m}^{-2} \text{ d}^{-1}$ and $273 \pm 11 \text{ mg m}^{-2} \text{ d}^{-1}$ respectively. Effluxes in the pelagic zone were lower in the hot rainy season than in the cold dry season but the seasonal variation was not significant ($p > 0.50$).

However, Fig. 4 displays a decreasing trend of CO_2 efflux toward downstream. The annual efflux from the river channel was $1577 \text{ mg m}^{-2} \text{ d}^{-1}$ and $905 \text{ mg m}^{-2} \text{ d}^{-1}$ in mainstream and tributary respectively, which were significantly higher than that in reservoir area ($p < 0.50$). The efflux in R1 was very sensitive to the monsoon climate. During summer, the efflux in R1 was no more than $274 \text{ mg m}^{-2} \text{ d}^{-1}$ but it rapidly climbed to $2359 \text{ mg m}^{-2} \text{ d}^{-1}$ at the end of October. The efflux was kept above $6,000 \text{ mg m}^{-2} \text{ d}^{-1}$ in the winter and the high rate last till the next March. Hence, the difference in efflux between river and reservoir was more significant in dry season but less obvious in wet season.

Point D at the downstream of the dam shared similar average efflux ($341 \pm 158 \text{ mg m}^{-2} \text{ d}^{-1}$) with Point P3, which correspond with the results of $p\text{CO}_2$ (Table 1 & Fig. 2). The emission at the downstream was concentrated in summer and winter while it dropped below $300 \text{ mg m}^{-2} \text{ d}^{-1}$ in spring and oscillated between 200 and $300 \text{ mg m}^{-2} \text{ d}^{-1}$ in autumn. This contradicts the findings on many tropical reservoirs but consistent with the low $p\text{CO}_2$ in some mountainous reservoirs in eastern China. The areal efflux downstream of the dam was always lower than that from the epilimnion in the reservoir as degassing could occur when water passes through the turbine for electricity generation. It suggests that the carbon emission rate downstream of the dam relied on the position of the water inlet and source layer of the water passing through the turbine.

However, the littoral zone has the highest emission rates within the reservoir ($684 \pm 1153 \text{ mg m}^{-2} \text{ d}^{-1}$), although this value was less than one third of the efflux estimated for drawdown area in temperate reservoirs (Aufdenkampe et al., 2011; Li, Zhang et al., 2015). This finding was consistent with the higher $p\text{CO}_2$. In autumn the littoral zone has the highest $p\text{CO}_2$ as well as the efflux along the reservoir when the frequent water level fluctuated drastically. Yet the positive relation between the efflux and



the nutrient input showed that the outgassing rates were closely to the growth of phytoplankton ($p < 0.05$), macrophytes and the possibly the plants on dry land.

3.4 Diurnal Variation of CO₂ effluxes

The diurnal observation of effluxes in the littoral zone showed that the CO₂ efflux was much higher at night (from 19:00 to 7:00: averagely $495 \pm 178 \text{ mg m}^{-2} \text{ d}^{-1}$) than in the daytime (from 7:00 to 19:00: averagely $247 \pm 171 \text{ mg m}^{-2} \text{ d}^{-1}$) (Fig. 5 & Fig. 6). The trend was verified by the discontinuous efflux measurements in which the nocturnal CO₂ flux ($1012.29 \pm 1016.84 \text{ mg m}^{-2} \text{ d}^{-1}$) was higher than the daytime flux ($766.87 \pm 740.43 \text{ mg m}^{-2} \text{ d}^{-1}$). The phenomenon was also commonly recorded in Chinese reservoirs as respiration dominates the ecosystem when light was unavailable for photosynthesis (Liu et al., 2016; Peng et al., 2012; Schelker et al., 2016).

Nevertheless, there was no significant difference in pCO₂ between nighttime and daytime ($p > 0.50$). In Fig. 5, pCO₂ increased steadily with the average of $969 \text{ } \mu\text{atm}$ at night and $871 \text{ } \mu\text{atm}$ in daytime. However, there was drastic oscillation of efflux from 9pm to 11pm with the range span from $712 \text{ mg m}^{-2} \text{ d}^{-1}$ to $69 \text{ mg m}^{-2} \text{ d}^{-1}$. Before 8pm, the efflux was kept below $400 \text{ mg m}^{-2} \text{ d}^{-1}$ but was above $450 \text{ mg m}^{-2} \text{ d}^{-1}$ after 0:30 in the midnight.

The insignificant difference in pCO₂ between day and night might be resulted from the little variation of pH. The pH was averagely 8.21 with the range no more than 0.28. But slightly decrease in pH was found at night, which lead to an increase of pCO₂ and the efflux. The water temperature increases from 13:00 to 19:30 while keep decreasing after 22:00. As the air temperature kept decreasing throughout the sampling period, the water was heated before 24:00 and start to loss heat to the atmosphere afterward. The alkalinity dropped from 15:00 to 19:30 while reverse the trend since 20:00. With a mean value of $2904 \text{ } \mu\text{g/L}$, the alkalinity reflects a similar variation trend as the pCO₂. Like the pH, the conductivity also varied little with the value ranged from $527.7 \text{ } \mu\text{S/cm}$ to $540.8 \text{ } \mu\text{S/cm}$. The wind speed was higher in the daytime with the maximum (3.5 m/s) took place in 16:30 while in the nighttime the sampling point was dominated by calm wind condition.

4 Discussion

4.1 Damming Effect on Carbon Evasion in the Upper Mekong River

In this study, CO₂ efflux from pristine river channel was much higher than that from reservoir surface, suggesting impounding did not increase CO₂ emission from the river. The CO₂ emission rates from reservoir surface was comparable to hypereutrophic natural lakes (Xing et al., 2005). No drastic increase of CO₂ emissions was found in the four-year-old reservoir. Even in the river channel, the highest effluxes were close to the effluxes from temperate reservoirs (Huttunen et al., 2002) and much lower than the tropical reservoirs (Abril et al., 2005; Fearnside, 1997; Guérin et al., 2006). There are multiple reasons for the low carbon effluxes. First, the upper Mekong River drains through the Tibetan Plateau and a narrow valley before it feeds into the GGQ. Because of poor vegetation in the catchment and intense precipitation during the rainy season, the catchment hardly



sustains fertile soil or provides abundant organic carbon for decomposition even in wet seasons. Shortage of the substrates for mineralization limits the production of carbon dioxide and thus the efflux. Secondly, damming the river greatly extend the water retention time and the riverine ecosystem gradually evolved into a limnetic ecosystem (Thornton et al., 1990). The extended water retention time in the pelagic zone of reservoirs was suitable for the development of phytoplankton communities.

5 When light, nutrient and temperature was favourable, intense photosynthesis will consume the CO_2 dissolved in surface water and lower the emission rates (Yu et al., 2009). In extreme cases like algae bloom, surface water tends to absorb CO_2 from the atmosphere (Pacheco et al., 2014). Thus, the valley-type reservoir exhibited a decreasing trend from river toward the dam in pCO_2 and the outgassing rates (Liu et al., 2009; Liu et al., 2014; Mei et al., 2011). Anthropogenic nutrient input can accelerate the process of eutrophication. With abundant nitrogen and phosphorous input from sewage, the outgassing rates can be even

10 decreased to a low level as natural lake or even become negative (Guo et al., 2011; Ran et al., 2011).

However, the CO_2 effluxes in this study correlated more closely to the physical and environmental factors rather than the biological factors. CO_2 evasion from the pelagic zone was largely insensitive to allochthonous organic carbon degradation in this study (Fig. 7). Higher carbon emission rates occurred in the cold dry season, which contradicts the pattern found in some other large valley-type reservoirs where rainfalls not only brings plenty of organic carbon but also increase flow velocity (Li

15 & Zhang, 2014; Zhao et al., 2013). Warmer climate also accelerates bacterial respiration (Åberg et al., 2010; Del Giorgio & Williams, 2005) and decreases solubility of carbon dioxide, thus enhancing the effluxes.

On the contrary, the effluxes in GGQ display a negative relation to the water temperature ($p < 0.01$, $\text{efflux} = -13.074 \cdot \text{Temp} + 544.374$, $R^2 = 0.260$). From Fig. 7, it can be seen that the reservoir had high effluxes when the temperature gradient between inflow water and reservoir surface water was larger, which suggests that this deviation from traditional

20 pattern was possibly related to the physical mixing process of inflow water and reservoir water. Seasonal variation of physiochemical property of inflow water and anti-season operation of reservoir could affect the hydrological condition of the water column in reservoir and thus the evasion of greenhouse gases (Striegl & Michmerhuizen, 1998). Even though in rainy season intense precipitation could bring plenty of sediments with organic matter, the turbid water might be discharged directly to the downstream for electricity, because of the relatively small storage capacity of the reservoir. The inflow water with

25 sediments, was heavier and colder than the reservoir water, thus it plunged into the water column in reservoir and became an underflow (turbid flow). The reservoir surface was less affected by the underflow and maintained a relatively stable emission rate (F. Pacheco et al., 2014) as continued water discharging allowed little time for mineralization of organic carbon (Assireu et al., 2011; Senturk, 1994). But in the dry season, the clean inflow water was lighter than the reservoir water, thus it joins the reservoir as surface flow. In Fig. 4, data shows that the inflow water in winter was also richer in CO_2 than the turbid inflow in

30 summer. When the water rich in CO_2 contacted the atmosphere directly, the gases could be directly diffuse into the air. Because the water kept losing CO_2 to the atmosphere, the decreasing trend in effluxes toward downstream was more significant in winter (Fig. 4). Besides, impounding water extended the water retention time in dry season, leaving more time for mineralization of organic carbon. To conclude, due to this difference in physical mixing process and availability of CO_2 , the



surface water tended to release more CO_2 in the dry season when water became colder in both inflow water and surface water in reservoir (Fig. 7). The underflow in the rainy season possibly also mix and aerate the water in the reservoir and thus impeded the formation of stratification. It was implied in the earlier studies that during stratification water from anoxic hypolimnion would be rich in carbon dioxide and was likely to release large amount of carbon dioxide when it passed the turbine (Mendonça et al., 2012), leading to intense emissions at the downstream river channel (Abril et al., 2005; Guérin et al., 2006; Wang et al., 2011). But emission rates at the downstream was largely dependent on positioning of water outlet of the dam. Comparison of the physiochemical properties of water at the upstream and downstream suggests that the water used for electricity generation in GGQ was mostly from epilimnion. Consequently, the efflux in the downstream was constraint and showed a similar seasonal variation to the reservoir surface water.

The littoral zone (or drawdown area) displayed much higher effluxes than the pelagic zone, especially in autumn and winter. The littoral zone has always been identified as a hotspot of carbon emission (Chen et al., 2009; Yang et al., 2012; Yang, 2011) since seasonal flooding could trigger anaerobic decomposition of dead macrophytes and produce greenhouse gases. Hence, it is believed that the frequent fluctuation of water level could deposit large amount of sediments as well as deadwoods on the relatively flat littoral zones. Decomposition of deadwoods tend to release organic acids to the water and lower the pH. As a result, the pCO_2 rises and more gases will be degassed out of the air-water interface. Furthermore, as the littoral zone was located in the transition zone of a reservoir, rich nutrients input as well as reduced turbidity facilitate growth of plants and macrophytes (Thornton et al., 1990). Some plants were able to release carbon dioxide even when they were submerged into the water. Thus, plant growth enhances respiration and CO_2 outgassing (Xu, 2013).

4.2 Extrapolation of the results and implication for future studies

The efflux from the pelagic zone and from the littoral zone was $352 \text{ mg m}^{-2} \text{ d}^{-1}$ and $684 \text{ mg m}^{-2} \text{ d}^{-1}$ respectively. Assuming the water level fluctuated frequently within 2.5m and the slope at the bank was 45° , the drawdown area covers an area of $1.81 \times 10^5 \text{ m}^2$. Hence the littoral zone can contribute 225.79g of carbon to the atmosphere, assuming it will be flooded in half of time. In terms of the emissions from the permanent flooded area, it is assumed that the area is $5,643,000 \text{ m}^2$. The carbon dioxide evaded from this area was 2.0t annually. Compared with the emission rate, the contribution from the littoral zone was actually negligible for its small area. However, if taking the diurnal variation into account, the annual carbon evasion reaches 3.0t as nocturnal effluxes was twice as in daytime. For one-hundred-year scale, the reservoir will release about 74kg CO_2 to the atmosphere, without concerning over the decaying rate. This estimation was within the range ($0.2 \sim 1994 \text{ kg CO}_2$ per MW/h) estimated by Räsänen et al. (2018) but almost double the median value. But it must be noticed that the CO_2 efflux will decrease as the reservoir ages (Abril et al., 2005; Barros et al., 2011). Accelerated eutrophication can possibly fix more CO_2 via photosynthesis (Liu et al., 2009).

Several problems have been noticed when computing the annual emission rate from GGQ. Despite its higher efflux, the drawdown area is negligible although the effluxes from reservoir always displayed high spatial heterogeneity (Barros et al.,



2011; Roland et al., 2010; Teodoru et al., 2011). To a larger scale the seasonal variation is also negligible as the effluxes in dry season was only $103 \text{ mg m}^{-2} \text{ d}^{-1}$ higher than in the rainy season. However, the higher effluxes in the nighttime must be taken into account. Measurement of the effluxes from reservoir surface have been usually limited by the pCO_2 samples collected in daytime and fail to capture a diurnal variation, though this variation has been fully recognized by a series of research (Liu et al., 2016; Peng et al., 2012; Schelker et al., 2016).

However, the sediment deposition must also be noticed when computing the long-term effect of reservoir on carbon cycle. As the farthest upstream reservoir along the Lancang cascades during the sampling period, GGQ also sequestered most of the sediments from the upstream catchments (Gao et al., 2017; Wang et al., 2011). It is very possible the reservoir cannot last for 100 years due to heavy silting problem (Fu & He, 2007), even though the sediment concentration decreased drastically after the upstream Miaowei Dam was completed. The reservoir was burying tons of organic carbon when it released carbon dioxide to the atmosphere (Mendonça et al., 2012; Mulholland & Elwood, 1982; Vörösmarty et al., 2003). Meanwhile the reservoirs could also sequester the nutrients in the rivers (Maavara et al., 2017; Maavara et al., 2015). Therefore, to evaluate the net effect of impoundments on carbon cycle, we need to quantify the organic carbon burial within the reservoir and finally build up a robust carbon budget. Besides, it was also expected the finding in spatial heterogeneity and seasonal variation of the effluxes from GGQ could help to extrapolate the carbon emissions from reservoirs to broader scale.

5 Conclusion

The epilimnion of the GGQ was supersaturated with CO_2 and a potential carbon source to the atmosphere. The results show that the reservoir tends to release 3.0 tons of CO_2 to the atmosphere annually. The effluxes from reservoir area was $408 \text{ mg m}^{-2} \text{ d}^{-1}$ and $305 \text{ mg m}^{-2} \text{ d}^{-1}$ in the dry season and rainy season respectively while the river channel exhibited an efflux of $2168 \text{ mg m}^{-2} \text{ d}^{-1}$ and $374 \text{ mg m}^{-2} \text{ d}^{-1}$ in these two seasons. The emission rate was much lower in river channel than in the reservoir area. The anti-season operation and difference in physiochemical properties between inflow water and reservoir surface water resulted in higher effluxes in cold dry season and lower emissions in warm wet season. The underflow in wet season was maintained and flushed the allochthonous organic carbon to the downstream, allowing little time for mineralization and limited effect on the emission rates from reservoir surface while the lighter overflow with higher pCO_2 in the dry season release more CO_2 . Emissions at the downstream the dam was also not limited as surface water, instead of hypolimnion water was used for generating electricity. However, the littoral zone suffering frequent fluctuation of water level was identified as a potential hotspot of CO_2 emissions. Flat topography and daily flooding could lead to accumulation of the deadwoods and resuspension of the deposited fine sediments, aerate the water and enhance the respiration rate. But its contribution to the total annual emission could be limited for its small area. Yet due to the significant diel variation, the total emissions from the reservoir might be increased by a half, when taking the nocturnal effluxes into account. Low effluxes in the daytime might be offset by the carbon absorption via photosynthesis. This pattern was rarely found in the mountainous valley-type reservoir and we hope



the future research could investigate more about the carbon sequestration within the reservoir to clarify whether the reservoir is a carbon sink or source.

5 Acknowledgements

The research leading to these results has received funding from the National Natural Science Foundation of China (Grant No. 41571032) and financial support from National Natural Science Foundation of China (Grant No. 91547110).

10 References

- Åberg, J., Jansson, M., & Jonsson, A. (2010). Importance of water temperature and thermal stratification dynamics for temporal variation of surface water CO₂ in a boreal lake. *Journal of Geophysical Research: Biogeosciences*, 115(G2), n/a-n/a. doi:10.1029/2009JG001085
- 15 Abril, G., Guérin, F., Richard, S., Delmas, R., Galy-Lacaux, C., Gosse, P., . . . Matvienko, B. (2005). Carbon dioxide and methane emissions and the carbon budget of a 10-year old tropical reservoir (Petit Saut, French Guiana). *Global biogeochemical cycles*, 19(4).
- Assireu, A., Alcântara, E., Novo, E., Roland, F., Pacheco, F., Stech, J., & Lorenzetti, J. (2011). Hydro-physical processes at the plunge point: an analysis using satellite and in situ data. *Hydrology and Earth System Sciences*, 15(12), 3689.
- 20 Aufdenkampe, A. K., Mayorga, E., Raymond, P. A., Melack, J. M., Doney, S. C., Alin, S. R., . . . Yoo, K. (2011). Riverine coupling of biogeochemical cycles between land, oceans, and atmosphere. *Frontiers in Ecology and the Environment*, 9(1), 53-60.
- Barros, N., Cole, J. J., Tranvik, L. J., Prairie, Y. T., Bastviken, D., Huszar, V. L., . . . Roland, F. (2011). Carbon emission from hydroelectric reservoirs linked to reservoir age and latitude. *Nature Geoscience*, 4(9), 593-596.
- 25 Battin, T. J., Luyssaert, S., Kaplan, L. A., Aufdenkampe, A. K., Richter, A., & Tranvik, L. J. (2009). The boundless carbon cycle. *Nature Geoscience*, 2(9), 598-600.
- Cole, J. J., Caraco, N. F., Kling, G. W., & Kratz, T. K. (1994). Carbon dioxide supersaturation in the surface waters of lakes. *Science*, 265(5178), 1568-1570.
- Cole, J. J., Prairie, Y. T., Caraco, N. F., McDowell, W. H., Tranvik, L. J., Striegl, R. G., . . . Middelburg, J. J. (2007). Plumbing the global carbon cycle: integrating inland waters into the terrestrial carbon budget. *Ecosystems*, 10(1), 172-185.



- De Lima, I. B. T., de Moraes Novo, E. M. L., Ballester, M. V. R., & Ometto, J. P. (1998, 1998). Methane production, transport and emission in Amazon hydroelectric plants.
- Deemer, B. R., Harrison, J. A., Li, S., Beaulieu, J. J., DelSontro, T., Barros, N., . . . Vonk, J. A. (2016). Greenhouse gas emissions from reservoir water surfaces: a new global synthesis. *Bioscience*, 66(11), 949-964.
- 5 Del Giorgio, P. A., & Williams, P. J. I. B. (2005). *Respiration in aquatic ecosystems*: Oxford University Press, USA.
- Fearnside, P. M. (1997). Greenhouse-gas emissions from Amazonian hydroelectric reservoirs: The example of Brazil's Tucuruí Dam as compared to fossil fuel alternatives. *Environmental conservation*, 24(01), 64-75.
- Fu, K., & He, D. (2007). Analysis and prediction of sediment trapping efficiencies of the reservoirs in the mainstream of the Lancang River. *Chinese Science Bulletin*, 52(2), 134-140.
- 10 Gao, Q., Tao, Z., Zhang, S., Xie, C., Lin, P., & Mao, H. (2017). The Damming Effects on the Dynamics of Riverine Carbon in a Mountainous River: A Case Study in the Zengjiang River, South China. *Quaternary Science*, 37(2), 331-342.
- Guérin, F., Abril, G., Richard, S., Burban, B., Reynouard, C., Seyler, P., & Delmas, R. (2006). Methane and carbon dioxide emissions from tropical reservoirs: significance of downstream rivers. *Geophysical Research Letters*, 33(21).
- Guo, J., Jiang, T., Li, Z., Chen, y., & Sun, Z. (2011). Analysis on partial pressure of CO₂ and influencing factors during spring
15 phytoplankton bloom in the backwater area of Xiaojiang River in Three Gorges Reservoir. *Advances in Water Science*, 22(6), 829-838.
- Holgerson, M. A., & Raymond, P. A. (2016). Large contribution to inland water CO₂ and CH₄ emissions from very small ponds. *Nature Geoscience*, 9(3), 222. doi:10.1038/ngeo2654
- Huai, C., Yuyuan, W., Xingzhong, Y., Yongheng, G., Ning, W., & Dan, Z. (2009). Methane emissions from newly created
20 marshes in the drawdown area of the Three Gorges Reservoir. *Journal of Geophysical Research - Atmospheres*, 114(D18), D18301. doi:10.1029/2009JD012410
- Huttunen, J. T., Väisänen, T. S., Hellsten, S. K., Heikkinen, M., Nykänen, H., Jungner, H., . . . Nenonen, O. S. (2002). Fluxes of CH₄, CO₂, and N₂O in hydroelectric reservoirs Lokka and Porttipahta in the northern boreal zone in Finland. *Global Biogeochemical Cycles*, 16(1), 3-13-17.
- 25 Kelly, C. A., & Hecky, R. E. (1993). Are Hydroelectric Reservoirs Significant Sources of Greenhouse Gases? *Ambio*, 22(4), 246-248.
- Kelly, C. A., Rudd, J. W., St Louis, V. L., & Moore, T. (1994). Turning attention to reservoir surfaces, a neglected area in greenhouse studies. *Eos, Transactions American Geophysical Union*, 75(29), 332-333.
- Lehner, B., & Döll, P. (2004). Development and validation of a global database of lakes, reservoirs and wetlands. *Journal of
30 Hydrology*, 296(1), 1-22.
- Lewis, E., Wallace, D., & Allison, L. J. (1998). Program developed for CO₂ system calculations: Carbon Dioxide Information Analysis Center, managed by Lockheed Martin Energy Research Corporation for the US Department of Energy Tennessee.



- Li, S., Lu, X., & Bush, R. T. (2013). CO₂ partial pressure and CO₂ emission in the Lower Mekong River. *Journal of Hydrology*, 504, 40-56.
- Li, S., & Zhang, Q. (2014). Partial pressure of CO₂ and CO₂ emission in a monsoon-driven hydroelectric reservoir (Danjiangkou Reservoir), China. *Ecological Engineering*, 71, 401-414.
- 5 Li, S., Zhang, Q., Bush, R. T., & Sullivan, L. A. (2015). Methane and CO₂ emissions from China's hydroelectric reservoirs: a new quantitative synthesis. *Environmental Science and Pollution Research*, 22(7), 5325-5339.
- Liu, C., Wang, F., Wang, Y., & Wang, B. (2009). Response of Aquatic Environment to River Damming. *Resources and Environment in the Yangtze Basin*, 18(4), 384-396.
- Liu, H., Zhang, Q., Katul, G. G., Cole, J. J., Chapin III, F. S., & MacIntyre, S. (2016). Large CO₂ effluxes at night and during
10 synoptic weather events significantly contribute to CO₂ emissions from a reservoir. *Environmental Research Letters*, 11(6), 064001.
- Liu, W., Pu, J.-b., Yu, S., Zhang, C., Au, Y.-y., Yuan, D.-x., . . . Tang, W. (2014). Preliminary Research on the Feature of Dissolved Inorganic Carbon in Wulixia Reservoir in Summer, Guangxi, China (in Chinese). *Environmental science*, 35(8), 2959-2966.
- 15 Maavara, T., Lauerwald, R., Regnier, P., & Van Cappellen, P. (2017). Global perturbation of organic carbon cycling by river damming. *Nature communications*, 8.
- Maavara, T., Parsons, C. T., Ridenour, C., Stojanovic, S., Dürr, H. H., Powley, H. R., & Van Cappellen, P. (2015). Global phosphorus retention by river damming. *Proceedings of the National Academy of Sciences*, 112(51), 15603-15608.
- Mei, H., Wang, F., Yao, C., & Wang, B. (2011). Diffusion Flux of Partial Pressure of Dissolved Carbon Dioxide in Wanan
20 Reservoir in Spring. *Environmental science*, 32(1), 58-63.
- Mendonça, R., Barros, N., Vidal, L. O., Pacheco, F., Kosten, S., & Roland, F. (2012). Greenhouse Gas Emissions from Hydroelectric Reservoirs: What Knowledge Do We Have and What is Lacking? In G. Liu (Ed.), *Greenhouse Gases - Emission, Measurement and Management*.
- Mendonça, R., Kosten, S., Sobek, S., Barros, N., Cole, J. J., Tranvik, L., & Roland, F. (2012). Hydroelectric carbon
25 sequestration. *Nature Geoscience*, 5(12), 838-840.
- MEP. (1989). Ministry of Environmental Protection of People's Republic of China. GB11893-89. In *Water Quality-Determination of total phosphorous: Ammonium molybdate spectrophotometric method*. Beijing: Standards Press of China.
- MEP. (2012). Ministry of Environmental Protection of People's Republic of China, HJ636-2012. In *Water Quality - Determination of total nitrogen: Alkaline potassium persulfate digestion - UV spectrometric method*. Beijing: Standards Press
30 of China.
- Mulholland, P. J., & Elwood, J. W. (1982). The role of lake and reservoir sediments as sinks in the perturbed global carbon cycle. *Tellus*, 34(5), 490-499.



- Pacheco, F., Soares, M., Assireu, A., Curtarelli, M., Roland, F., Abril, G., . . . Ometto, J. (2014). River inflow and retention time affecting spatial heterogeneity of chlorophyll and water–air CO₂ fluxes in a tropical hydropower reservoir. *Biogeosciences Discussions*, 11(6), 8531-8568.
- Pacheco, F. S., Roland, F., & Downing, J. A. (2014). Eutrophication reverses whole-lake carbon budgets. *Inland waters*, 4(1), 41-48. doi:10.5268/IW-4.1.614
- Peng, X., Wang, B., Liu, C., Liu, X., & Wang, F. (2012). Diurnal variations of pCO₂ in relation to environmental factors in the cascade reservoirs along the Wujiang River, China. *Chinese Journal of Geochemistry*, 31(1), 41-47.
- Qu, B., Aho, K. S., Li, C., Kang, S., Sillanpää, M., Yan, F., & Raymond, P. A. (2017). Greenhouse gases emissions in rivers of the Tibetan Plateau. *Scientific reports*, 7(1), 16573.
- Ran, J., Lin, C., Guo, J., Chen, Y., & Jiang, T. (2011). Spatial and temporal variation of carbon dioxide partial pressure over the Xiaojiang River backwater area of the Three Gorges Reservoir. *Resource and Environment in the Yangtze Basin*, 20(8), 976-982.
- Räsänen, T. A., Varis, O., Scherer, L., & Kummu, M. (2018). Greenhouse gas emissions of hydropower in the Mekong River Basin. *Environmental Research Letters*.
- Raymond, P. A., Hartmann, J., Lauerwald, R., Sobek, S., McDonald, C., Hoover, M., . . . Humborg, C. (2013). Global carbon dioxide emissions from inland waters. *Nature*, 503(7476), 355-359.
- Regnier, P., Andersson, A. J., Arndt, S., Arnosti, C., Borges, A. V., Dale, A. W., . . . Luyssaert, S. (2013). Anthropogenic perturbation of the carbon fluxes from land to ocean. *Nature Geoscience*, 6(8), 597. doi:10.1038/ngeo1830
- Roland, F., Vidal, L., Pacheco, F., Barros, N., Assireu, A., Ometto, J. H. B., . . . Cole, J. (2010). Variability of carbon dioxide flux from tropical (Cerrado) hydroelectric reservoirs. *Aquatic Sciences*, 72(3), 283-293. doi:10.1007/s00027-010-0140-0
- Rudd, J. W., Hecky, R., Harris, R., & Kelly, C. (1993). Are hydroelectric reservoirs significant sources of greenhouse gases.
- Schelker, J., Singer, G. A., Ulseth, A. J., Hengsberger, S., & Battin, T. J. (2016). CO₂ evasion from a steep, high gradient stream network: importance of seasonal and diurnal variation in aquatic pCO₂ and gas transfer. *Limnology and Oceanography*, 61(5), 1826-1838.
- Senturk, F. (1994). *Hydraulics of dams and reservoirs*. Highlands Ranch, Colo: Water Resources Publications.
- Shi, W., Chen, Q., Yi, Q., Yu, J., Ji, Y., Hu, L., & Chen, Y. (2017). Carbon Emission from Cascade Reservoirs: Spatial Heterogeneity and Mechanisms. *Environmental science & technology*, 51(21), 12175-12181.
- Striegl, R. G., & Michmerhuizen, C. M. (1998). Hydrologic influence on methane and carbon dioxide dynamics at two north-central Minnesota lakes. *Limnology and Oceanography*, 43(7), 1519-1529.
- Tadonleke, R. D., Marty, J. m., & Planas, D. (2012). Assessing factors underlying variation of CO₂ emissions in boreal lakes vs. reservoirs. *FEMS microbiology ecology*, 79(2), 282-297.
- Thornton, K. W., Kimmel, B. L., & Payne, F. E. (1990). *Reservoir limnology: ecological perspectives*: John Wiley & Sons.



- Tranvik, L. J., Downing, J. A., Cotner, J. B., Loiselle, S. A., Striegl, R. G., Ballatore, T. J., . . . Knoll, L. B. (2009). Lakes and reservoirs as regulators of carbon cycling and climate. *Limnology and Oceanography*, 54(6), 2298-2314.
- Tremblay, A., Varfalvy, L., Roehm, C., & Garneau, M. (2005). *Greenhouse gas emissions-fluxes and processes*: Springer.
- Varis, O., Kumm, M., Härkönen, S., & Huttunen, J. T. (2012). Greenhouse gas emissions from reservoirs. In *Impacts of Large Dams: A Global Assessment* (pp. 69-94): Springer.
- Vincent, L. S. L., Carol, A. K., Eric, D., John, W. M. R., & David, M. R. (2000). Reservoir surfaces as sources of greenhouse gases to the atmosphere: A global estimate. *Bioscience*, 50(9), 766.
- Vörösmarty, C. J., Meybeck, M., Fekete, B., Sharma, K., Green, P., & Syvitski, J. P. (2003). Anthropogenic sediment retention: major global impact from registered river impoundments. *Global and Planetary Change*, 39(1), 169-190.
- Wang, B., Wang, Y., Wang, F., Liu, X., Liu, C.-Q., Guan, J., & Yu, Y. (2011). Carbon dioxide emission from surface water in cascade reservoirs–river system on the Maotiao River, southwest of China. *Atmospheric Environment*, 45(23), 3827-3834. doi:10.1016/j.atmosenv.2011.04.014
- Xing, Y., Xie, P., Yang, H., Ni, L., Wang, Y., & Rong, K. (2005). Methane and carbon dioxide fluxes from a shallow hypereutrophic subtropical Lake in China. *Atmospheric Environment*, 39(30), 5532-5540.
- Xu, Z. (2013). *Study of Carbon Dioxide and nitrous oxide emissions from Ecosystems of Different Elevations in a Typical Water Level Fluctuating Zone in Three Gorges Reservoir*. Southwest University,
- Yang, L., Lu, F., Wang, X., Duan, X., Song, W., Sun, B., . . . Zheng, F. (2012). Surface methane emissions from different land use types during various water levels in three major drawdown areas of the Three Gorges Reservoir. *Journal of Geophysical Research: Atmospheres* (1984–2012), 117(D10).
- Yang, M. (2011). *Spatial-temporal Variation of Greenhouse Gas Flux and Its Environmental Factors at Miyun Water Reservoir* [D]. Beijing Forestry University,
- Yu, Y., Wang, F., Wang, B., & Li, G. (2009). Response of Dissolved Inorganic Carbon and Its Isotopic Spatial and Temporal Characteristics to the Earlier Reservoir Process: A Case Study on a New Reservoir (Hongjiadu) (in Chinese). *Acta Mineralogica Sinica*, 29(2), 268-274.
- Zhao, Y., Wu, B. F., & Zeng, Y. (2013). Spatial and temporal patterns of greenhouse gas emissions from Three Gorges Reservoir of China. *Biogeosciences*, 10(2), 1219-1230.

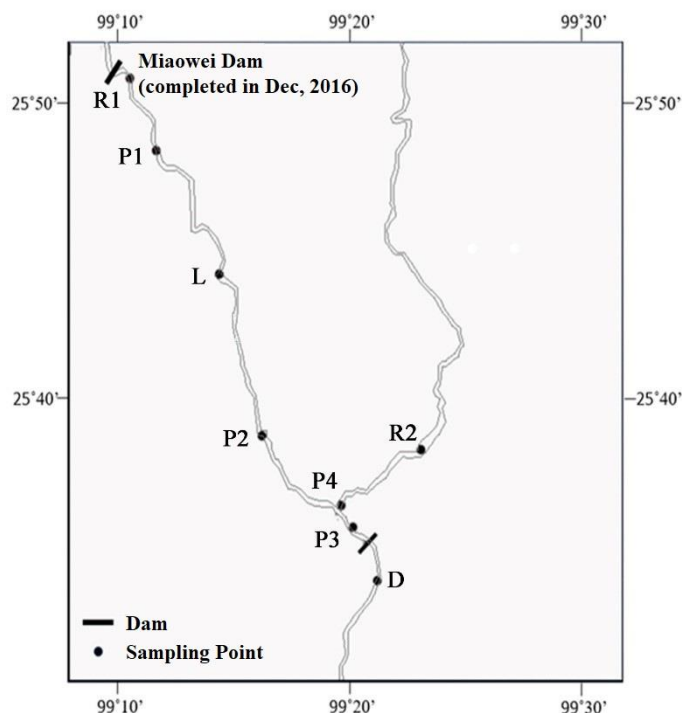


Figure 1 Sampling points in the Gongguoqiao Reservoir and its position within the Mekong River Basin. Point L1 is downstream the Miaowei Dam which was completed in Dec, 2016. Point R1 and R2 was in the river channel with flow velocity. Point P1, P2, P3 and P4 were in the reservoir without flow velocity. Point D was at the downstream of the reservoir. Point R2 and P4 were in the tributary the Bijiang River while all the other points were in the mainstream of Mekong River (or Lancang River).

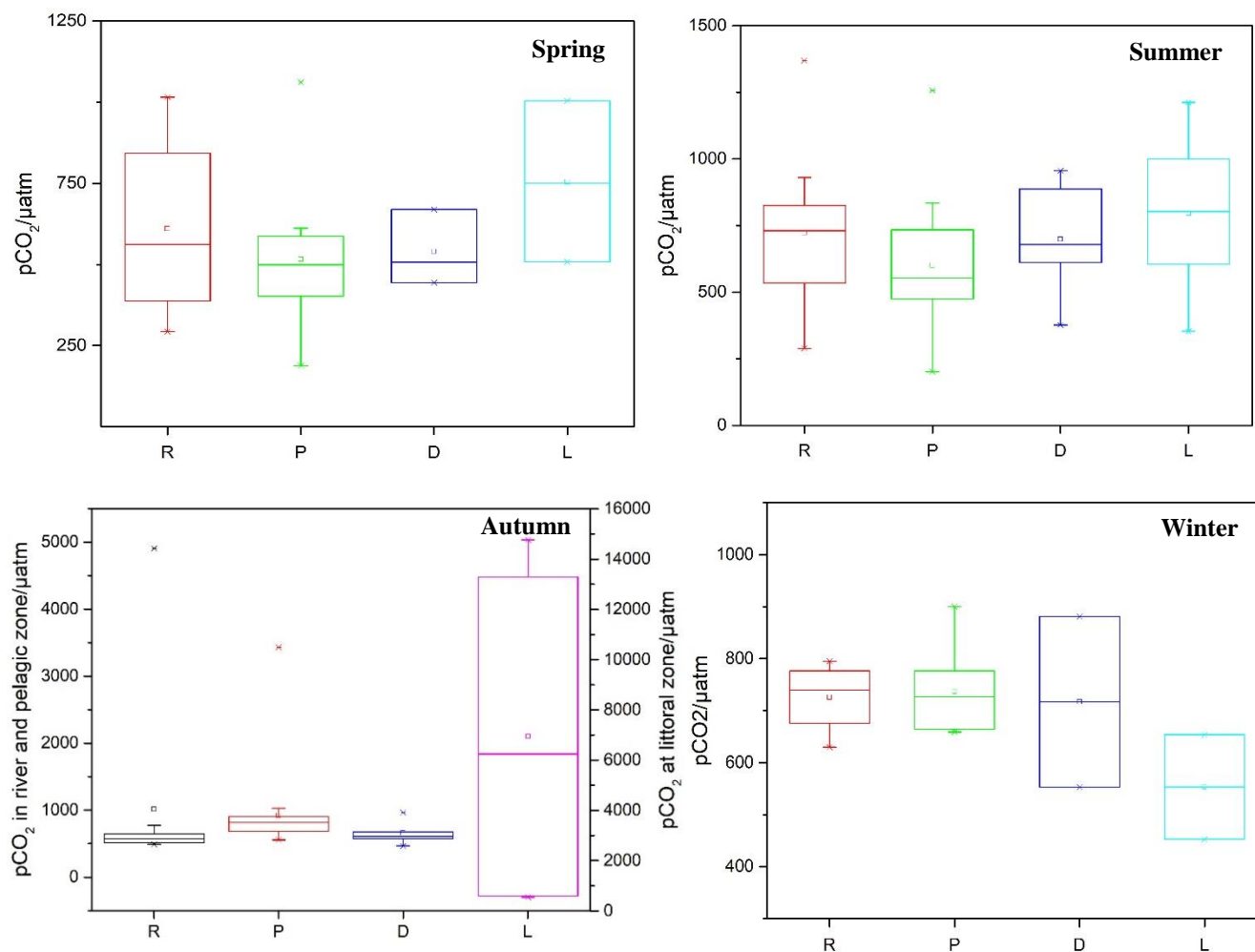


Figure 2 Box Plots of $p\text{CO}_2$ in the rivers (R), permanent flooded area of the reservoir (P), downstream (D) and littoral zone (L) in the four seasons. Notice that the scale of $p\text{CO}_2$ at the littoral zone in autumn was shown on the scale of right hand side. The vertical line indicates the 1.5 interquartile range. The points outside the range was considered outliers and are represented by little cross. Horizontal line refers to the median value while the little squares refers to the average. This could be applied to all the box plots below.

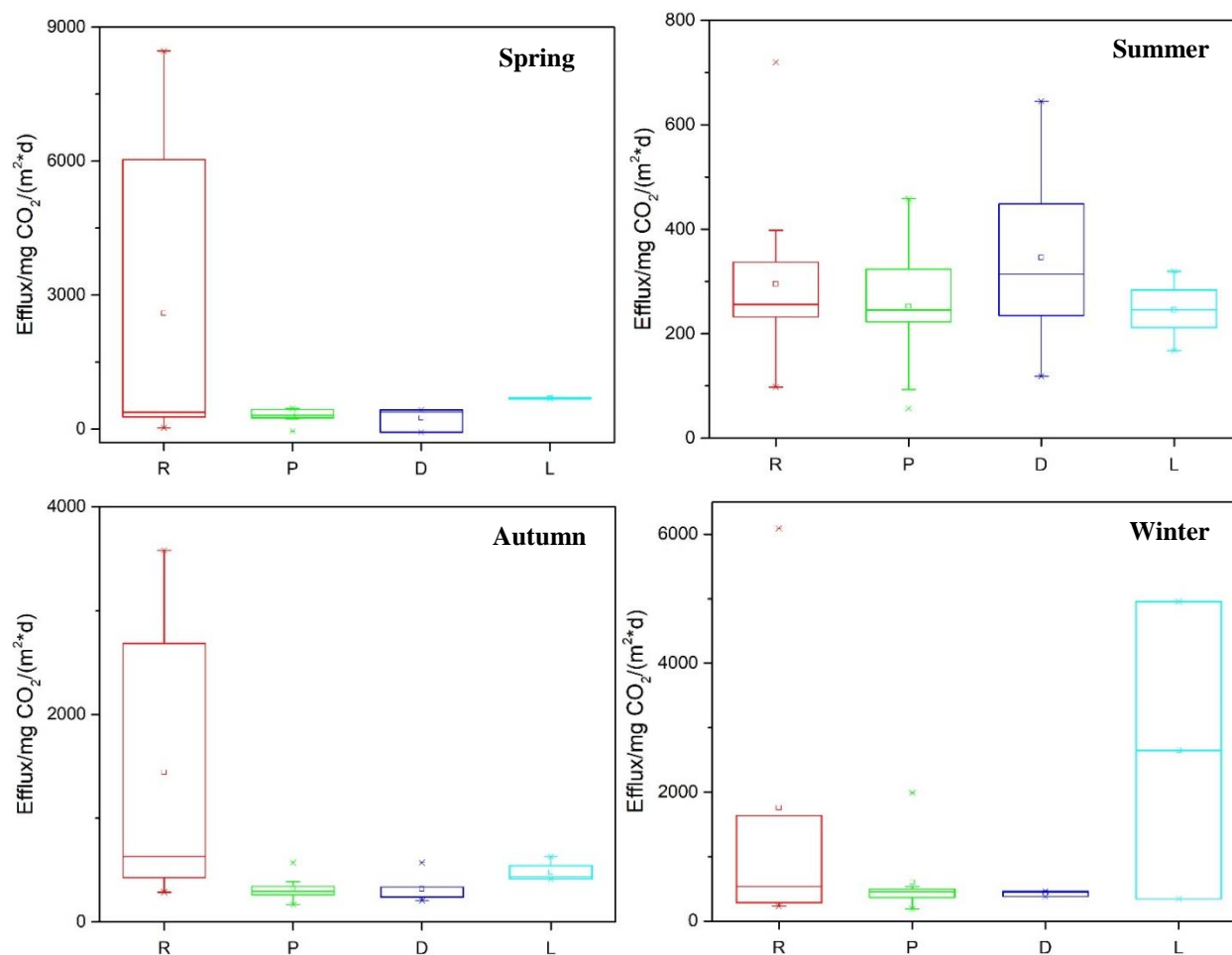


Figure 3 Box plots of the measured CO₂ effluxes in the four seasons. The legends are the same as Fig. 2.

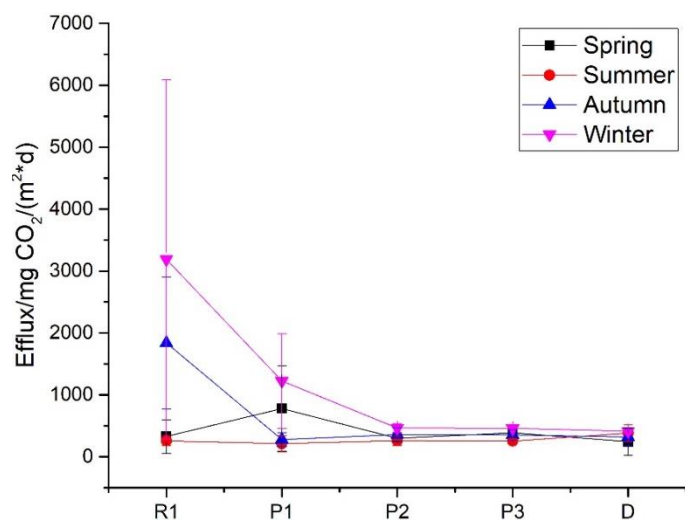


Figure 4 Longitudinal variation in effluxes along the mainstream in different seasons. The points and error bar refers to mean value and standard deviation respectively.

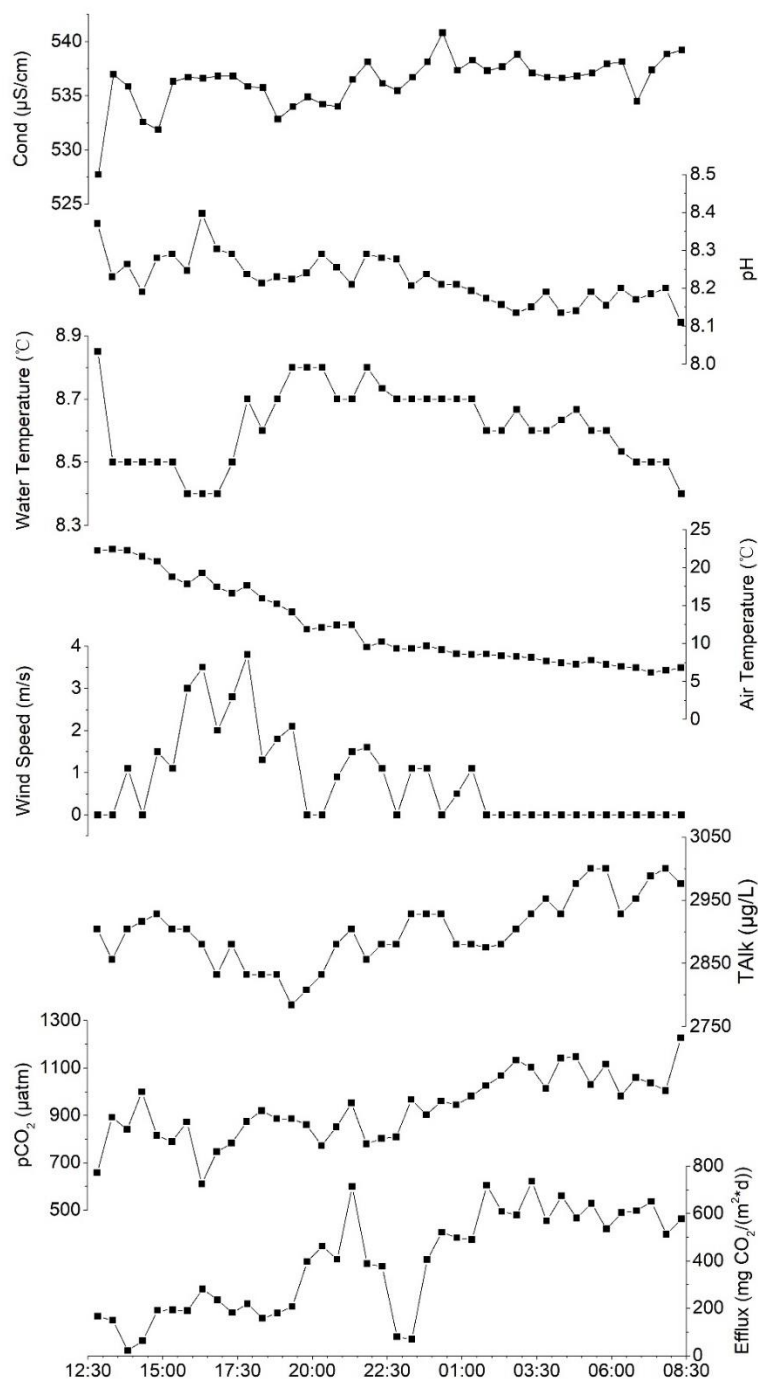


Figure 5 Diurnal variation of the water environment (including conductivity, pH, water temperature and total alkalinity), atmospheric environment (air temperature and wind speed) pCO₂ and efflux.

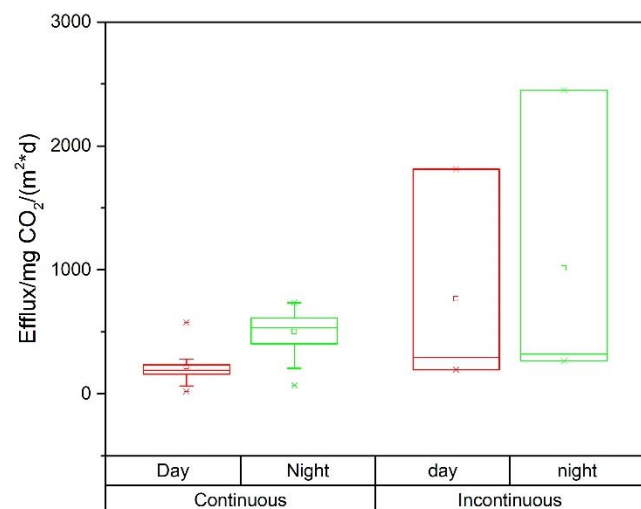


Figure 6 Comparison in effluxes between daytime and night via continuous samples (left panel) and incontinuous samples (right panel)

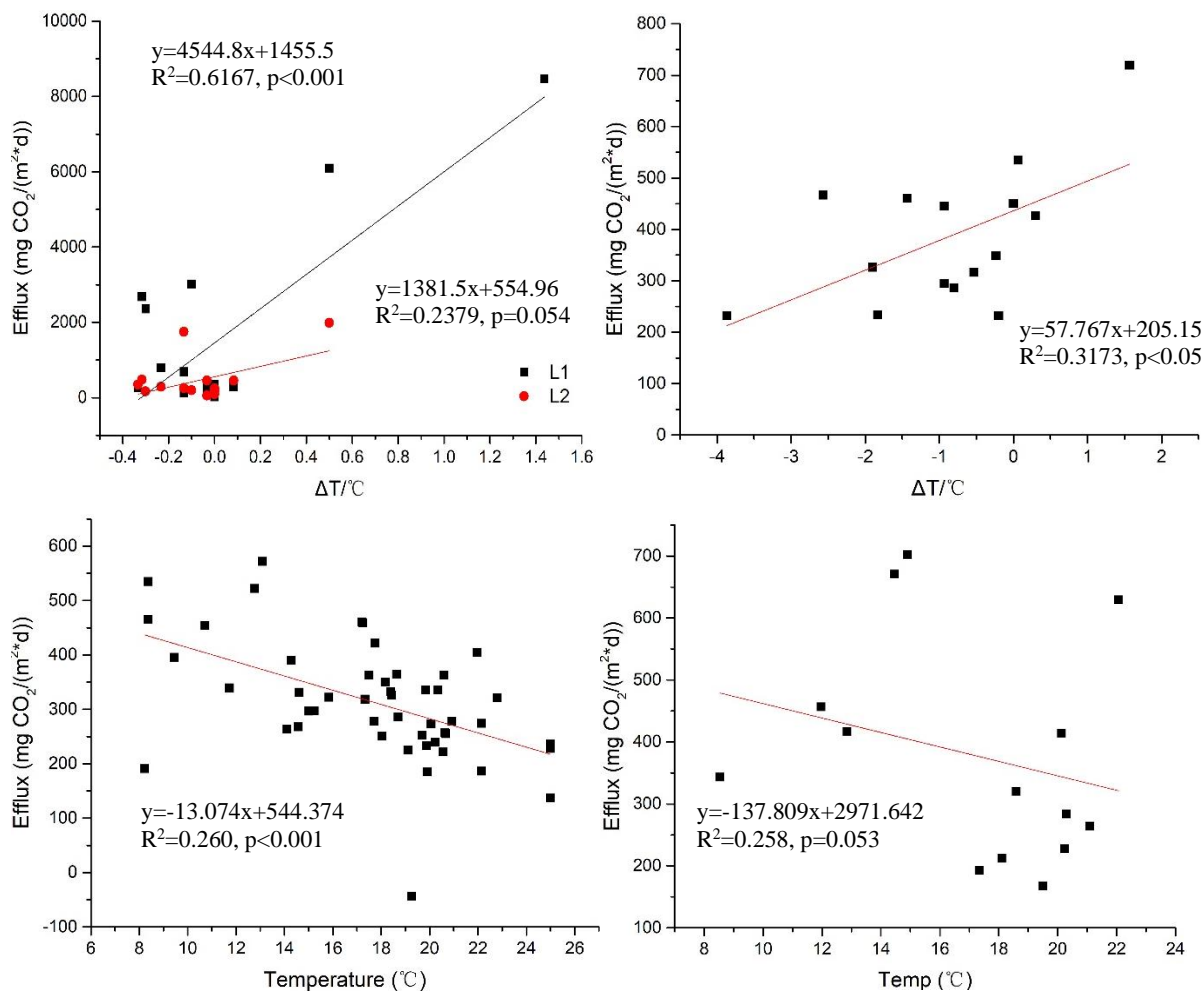


Figure 7 Positive correlations between water temperature gradient (TR1-P1 or TR2-P4) and measured effluxes in the riverine zone on the mainstream (upper left) and on the tributary (upper right) and negative correlations between water temperature and effluxes in the pelagic zone (lower left) and in the littoral zone (lower right). Notice that two extreme values were excluded out in the linear regression in the upper right panel.



Table 1 Mean temperature (Temp), pH, total alkalinity (Talk), conductivity (Cond), dissolved oxygen (DO), partial pressure of CO₂ (pCO₂), concentration of chlorophyll a (Chl a), concentration of total nitrogen (TN) and total phosphorous (TP) of sampling points

	Temp/°C			pH			Cond/μS/cm			DO/mg/L			Talk/μg/L		
	MIN	MAX	MED	MIN	MAX	MED	MIN	MAX	MED	MIN	MAX	MED	MIN	MAX	MED
R1	8.4	20.5	16.9	7.47	9.73	8.40	296.2	536.4	355.4	8.08	19.33	8.93	1696	3036	2608
R2	8.3	21.1	19.2	8.09	9.50	8.35	159.8	437.7	295.0	4.61	20.16	7.97	1888	3456	2508
P1	8.3	20.5	17.1	7.63	10.13	8.38	256.6	540.4	352.5	8.03	10.05	8.81	1712	2928	2486
P2	8.4	25.0	17.8	8.03	9.93	8.35	214.2	537.2	330.5	7.94	9.32	8.66	1528	2928	2338
P3	8.4	25.0	18.6	8.05	10.77	8.28	253.2	462.9	333.0	7.49	8.83	8.30	1800	2772	2262
P4	8.2	25.0	19.6	8.08	12.70	8.34	259.4	494.2	343.6	7.63	9.87	7.90	1888	2928	2220
D	8.3	25.0	17.5	8.17	10.07	8.37	266.0	529.2	340.1	7.96	20.11	9.90	1784	3000	2508
L	8.5	22.1	18.1	7.00	13.53	8.34	275.4	539.4	357.7	6.77	9.07	8.49	1928	4320	2736



Table 1 Continued

	TN/mg/L			TP/mg/L			Chl a/mg/L			pCO ₂ /ppm		
	MIN	MAX	MED	MIN	MAX	MED	MIN	MAX	MED	MIN	MAX	MED
R1	0.04	1.40	0.51	0.01	0.73	0.12	0.73	2.34	0.99	293	4902	572
R2	0.20	4.47	0.69	0.01	1.65	0.30	0.75	2.09	1.15	289	1369	748
P1	0.04	1.66	0.51	0.01	0.65	0.04	0.61	2.68	1.01	237	3427	621
P2	0.04	2.30	0.59	0.01	0.52	0.02	0.75	1.68	0.92	201	1062	637
P3	0.04	1.59	0.65	0.01	0.49	0.02	0.62	1.84	0.95	448	1257	698
P4	0.04	2.78	0.79	0.01	0.12	0.02	0.61	1.18	0.99	188	1183	747
D	0.03	1.88	0.52	0.01	0.71	0.02	0.63	2.05	0.99	377	958	615
L	0.04	2.48	0.61	0.01	0.50	0.02	0.63	1.60	0.98	353	14764	750